ENVIRONMENTAL RESEARCH
LETTERS

LETTER • OPEN ACCESS

Land cover change in low-warming scenarios may enhance the climate role of secondary organic aerosols

To cite this article: Marianne T Lund *et al* 2021 *Environ. Res. Lett.* **16** 104031

ENVIRONMENTAL RESEARCH
LETTERS

OPEN ACCESS

RECEIVED
9 May 2021

REVISED
23 August 2021

ACCEPTED FOR PUBLICATION
14 September 2021

PUBLISHED
6 October 2021

LETTER

Land cover change in low-warming scenarios may enhance the climate role of secondary organic aerosols

Marianne T Lund[1,*], **Alexandru Rap**[2], **Gunnar Myhre**[1], **Amund S Haslerud**[1] **and Bjørn H Samset**[1]

[1] CICERO Center for International Climate Research, Oslo, Norway
[2] School of Earth and Environment, University of Leeds, Leeds, United Kingdom
[*] Author to whom any correspondence should be addressed.

E-mail: m.t.lund@cicero.oslo.no

Keywords: secondary organic aerosol, land cover change, climate, land-based mitigation

Supplementary material for this article is available online

Abstract

Most socioeconomic pathways compatible with the aims of the Paris Agreement include large changes to land use and land cover. The associated vegetation changes can interact with the atmosphere and climate through numerous mechanisms. One of these is emissions of biogenic volatile organic compounds (BVOCs), which may lead to the formation of secondary organic aerosols (SOAs) and atmospheric chemistry changes. Here, we use a modeling framework to explore potential future global and regional changes in SOA and tropospheric ozone following idealized, large-scale vegetation perturbations, and their resulting radiative forcing (RF). Guided by projections in low-warming scenarios, we modify crop and forest cover, separately, and in concurrence with changes in anthropogenic emissions and CO_2 level. We estimate that increasing global forest cover by 30% gives a 37% higher global SOA burden, with a resulting forcing of -0.13 W m^{-2}. The effect on tropospheric ozone is relatively small. Large SOA burden changes of up to 48% are simulated for South America and Sub-Saharan Africa. Conversely, increasing crop cover at the expense of tropical forest, yields similar changes but of opposite sign. The magnitude of these changes is strongly affected by the concurrent evolution of anthropogenic emissions. Our land cover perturbations are representative of energy crop expansion and afforestation, two key mitigation measures in 1.5 °C compatible scenarios. Our results hence indicate that depending on the role of these two in the underlying mitigation strategies, scenarios with similar long-term global temperature levels could lead to opposite effects on SOA. Combined with the complexity of factors that control SOA, this highlights the importance of including BVOC effects in further studies and assessments of climate and air quality mitigation involving the land surface.

1. Introduction

Many mitigation pathways compatible with the Paris Agreement ambition to limit global warming to well below 2 °C above pre-industrial levels rely heavily on negative emission technologies, such as reforestation, afforestation and large-scale deployment of bioenergy with carbon capture and storage (Harper *et al* 2018, Rogelj 2018, Roe *et al* 2019). This in turn will entail significant changes to vegetation and other features of the terrestrial ecosystem (Popp *et al* 2017, Doelman *et al* 2018), that may feed back on the atmosphere and climate through a range of other physical, chemical and biological processes. Land cover change (LCC) can therefore have substantial impacts on the atmospheric energy budget and the hydrological cycle, on local to global scales (e.g. Mahmood *et al* 2014), sometimes with strong regional heterogeneity. For instance, loss of boreal forest cover has a cooling effect due to enhanced albedo, while tropical deforestation reduces evapotranspiration and increases sensible heat fluxes, resulting in surface warming (Bala *et al* 2007, Alkama and Cescatti 2016). Studies suggest that historical LCC has induced a net cooling impact through biogeophysical processes, which, although smaller than the impact of land-use CO_2 emissions over the same period on a global scale, has substantial influence on regional climate features, including

climate extremes (Pongratz *et al* 2010, Ghimire *et al* 2014, Lejeune *et al* 2017, Hirsch *et al* 2018).

In this study we focus on a possibly highly important, but often less well explored, mechanism of land-climate interactions: the emission of chemically reactive biogenic volatile organic compounds (BVOCs) and subsequent impacts on the atmospheric composition of aerosols and trace gases. Once in the atmosphere, BVOCs, of which isoprene is the dominating species, may affect oxidation chemistry, and hence tropospheric concentrations of ozone, a potent greenhouse gas and harmful air pollutant. The BVOC oxidation products also react to form secondary organic aerosol (SOA) (Claeys *et al* 2004, Kanakidou *et al* 2005, Carslaw *et al* 2010). SOA plays a marked role in the climate system through its ability to scatter and absorb solar radiation and influence the concentration of cloud condensation nuclei (CCN) through new particle formation or particle growth. Earlier studies have suggested that organic aerosol (OA), including SOA, are comparable in abundance to sulfate aerosol in the Northern Hemisphere and that SOA may be responsible for more than half the continental CCN (Jimenez *et al* 2009, D'Andrea *et al* 2013). However, despite significant recent advances, the SOA budget, and its contribution to the spread in indirect aerosol forcing estimates, remain uncertain (Carslaw *et al* 2013, Rap *et al* 2013, Shrivastava *et al* 2017, Zhu *et al* 2019, Sporre *et al* 2020).

The processes that control the terrestrial source of biogenic SOA are highly sensitive to climate, land cover and other environmental factors. For instance, rising surface temperatures drive increases in BVOC emissions and SOA loads, leading to negative radiative forcing (RF) and a cooling effect on the climate. This feedback mechanism has been explored through both modeling and observational studies (Paasonen *et al* 2013, Scott *et al* 2018a, Thornhill *et al* 2021). BVOC emission rates are also sensitive to the background CO_2 concentration, with most studies pointing to an isoprene inhibition effect with increasing CO_2 (Arneth *et al* 2007, Pacifico *et al* 2009, Tai *et al* 2013). Rap *et al* (2018) used a modeling approach to show that there is a strong positive ecosystem feedback between global BVOC emissions and plant productivity via diffuse radiation fertilization. Studies have also demonstrated significant variability in isoprene emissions due to environmental change over historical periods (Unger 2013, Chen *et al* 2018), and that changes in the abundance of SOA and ozone can make notable contributions to the net climate impact of historical LCC (Unger 2014, Scott *et al* 2017). Future changes in BVOC emissions and SOA are expected in response to warming and increased conversion of land, although the magnitude of the response varies significantly depending on scenario and methodological framework (Guenther *et al* 2006, Heald *et al* 2008, Ward *et al* 2014, Hantson *et al* 2017).

Many of the recent emission and socioeconomic pathways, the shared socioeconomic pathways (SSPs) (O'Neill *et al* 2014), project large land cover/land-use conversion, particularly following extensive use of land-based climate mitigation measures. However, the characteristics of the projected LCC can differ substantially even in scenarios with the same global temperature level, depending on the chosen mitigation strategy and the balance between afforestation/reforestation and expansion of bioenergy crops (Bertram *et al* 2018, Huppman *et al* 2018). Concurrently, global emissions of anthropogenic aerosols are projected to decline strongly, while background CO_2 concentrations will continue to increase towards the mid-21st century even in 1.5 °C compatible scenarios. The magnitude and sign of the consequent change in BVOC emissions (affecting SOA and ozone concentrations) in these scenarios are poorly quantified, but potentially of high relevance for global and regional climate.

In the following, we explore effects on global and regional atmospheric composition and energy balance resulting from contrasting, large-scale vegetation perturbations guided by total LCC in recent low-warming scenarios. We perform a series of model experiments with a state-of-the-art global chemical-transport model (CTM). Alternative land cover maps are constructed, keeping the land cover perturbations idealized with the aim of spanning a broad range of possible evolution across different regions. The resulting effect on BVOC emissions, SOA and ozone is simulated, delineating the impact of LLC from the influence of changing anthropogenic emissions, and the associated impact on the energy balance quantified.

2. Methods

We construct three main perturbations to large-scale vegetation, as well as a range of additional sensitivity experiments. The changes in SOA and tropospheric ozone caused by these perturbations are explored using the OsloCTM3 (Søvde *et al* 2012), which is driven by meteorological data from the European Center for Medium Range Weather Forecast (ECMWF) open integrated forecasting system (OpenIFS) and uses the 2.25° × 2.25° horizontal resolution with 60 vertical layers. The OsloCTM3 includes comprehensive treatment of tropospheric and stratospheric chemistry (Berntsen and Isaksen 1997, Søvde *et al* 2012), as well as modules for the main aerosol species (Lund *et al* 2018). The SOA parameterization, based on Chung and Seinfeld (2002), is documented by Hoyle *et al* (2007). A brief overview is given in the SI (available online at stacks.iop.org/ERL/16/104031/mmedia).

While the standard model configuration relies on offline data sets for BVOC emissions, we have here implemented the parameterization from the Model

of Emissions of Gases and Aerosols from Nature version 2.1 (MEGAN2.1) (Guenther *et al* 2012) in the OsloCTM3. MEGAN is driven by input of weather and land cover data and uses mechanistic algorithms to represent the major known processes that control biogenic emissions. We use ECMWF OpenIFS meteorological data, leaf area index derived from global inventory modeling and mapping studies normalized difference vegetation index (Zhu *et al* 2013), figure S1, and the plant function type (PFT) distribution from the Community Land Model version 4 (Lawrence *et al* 2011) combined with the PFT specific emission factors from MEGAN2.1. Anthropogenic and biomass burning emissions are taken from the Community Emission Data System (van Marle *et al* 2017, Hoesly *et al* 2018).

The RF of the changes in SOA and tropospheric ozone is calculated offline using two different radiative transfer models; SOCRATES (Edwards and Slingo 1996, Rap *et al* 2013) and Oslo-RTM (Myhre *et al* 2017). In SOCRATES, the forcing due to aerosol–radiation interactions (RFari) is estimated using the CLASSIC aerosol scheme (Bellouin *et al* 2011), while stratospherically-adjusted ozone RF is calculated using the fixed dynamic heating approximation (Rap *et al* 2015). RFari is also calculated with the Oslo-RTM using a multi-stream model with the discrete ordinate method (Stamnes *et al* 1988). Biogenic SOA is assumed to be purely scattering. Additionally, the Oslo-RTM is used to derive an estimate of the RF of aerosol–cloud interactions (RFaci), using the method by Quaas *et al* (2006) to account for the aerosol-induced change in cloud droplet concentration, which alter the cloud effective radius and thus the optical properties of the clouds. This method has been applied in earlier studies (e.g. Myhre *et al* 2017).

We perform a baseline, present-day (year 2014) run and a set of sensitivity experiments, modifying the vegetation cover but with fixed 2014 meteorological data (table 1). Each simulation is 1 year, with 6 months spin-up. Three experiments are performed where the total global forest or crop cover is increased by 30% compared to the baseline (with corresponding decrease in other PFTs). This number is based on end-of-century LCCs from present-day in two scenarios from the IAMC 1.5 °C Scenario Explorer hosted by IIASA (Huppman *et al* 2018), the 1p5C_Sust and 1p5C_early (figure S2), which have the same level of global warming but different underlying policies and assumptions (Bertram *et al* 2018). We assume instantaneous changes, i.e. we do not treat the dynamical transition to a new land cover distribution, but explore the role of biogenic SOA and ozone in this new state. Additionally, we perform experiments with a 15% increase in global cover forest and crop, more representative of mid-century changes, and an extreme case with a 50% increase.

Our updated vegetation maps are produced as follows: (a) in each grid cell where forest currently exist, the percentage cover is increased by the respective amount (15%, 30% or 50%) (up to a maximum of 100%); (b) the amount of crop and grass/shrub is then reduced by a corresponding amount. In a similar way, for an increase in crop cover, we reduce the forest and grass/shrub cover). In reality, not all grassland or forested areas are suited for agriculture, nor can forests be planted everywhere. However, here we aim to keep the perturbations idealized and hence primarily retain the present-day geographical land cover distribution. To test the effect of this constraint, we also perform an experiment where the 30% increase in crop cover only takes place at the expense of tropical forest (i.e. equivalent to a tropical deforestation case). Figure 1 shows the baseline distribution of forests, crop, and shrub/grass and the pattern of vegetation change in the 30% forest increase, 30% crop increase and deforestation experiments, while table S1 gives total cover for each of the three land cover types in each experiment.

For two of the vegetation perturbations, 30% forest and crop increase, we perform additional simulations where anthropogenic emissions of aerosols and precursor gases and background CO_2 concentrations are set to levels corresponding to a low

Table 1. Summary and description of experiments. Unless otherwise specified, the anthropogenic emissions and background CO_2 concentration are kept at the present-day (year 2014) levels. We focus particularly on the three scenarios in bold in the following sections.

Experiment	Description
Baseline	Present-day land cover
Forest15	15% increase in global forest cover
Forest30	**30% increase in global forest cover**
Forest50	50% increase in global forest cover
Forest30_SSP119anthro	Same as Forest30, but with year 2050 SSP1-1.9 anthropogenic emissions
Forest30_SSP119all	Same as Forest30, but with year 2050 SSP1-1.9 anthropogenic emissions and CO_2 concentration
Crop15	15% increase in global crop cover
Crop30	**30% increase in global crop cover**
Crop50	50% increase in global crop cover
Crop30_SSP119anthro	Same as Crop30, but with year 2050 SSP1-1.9 anthropogenic emissions
Crop30_SSP119all	Same as Crop30, but with year 2050 SSP1-1.9 anthropogenic emissions and CO_2 concentration
Deforest	**30% of tropical forest cover replaced by crop**

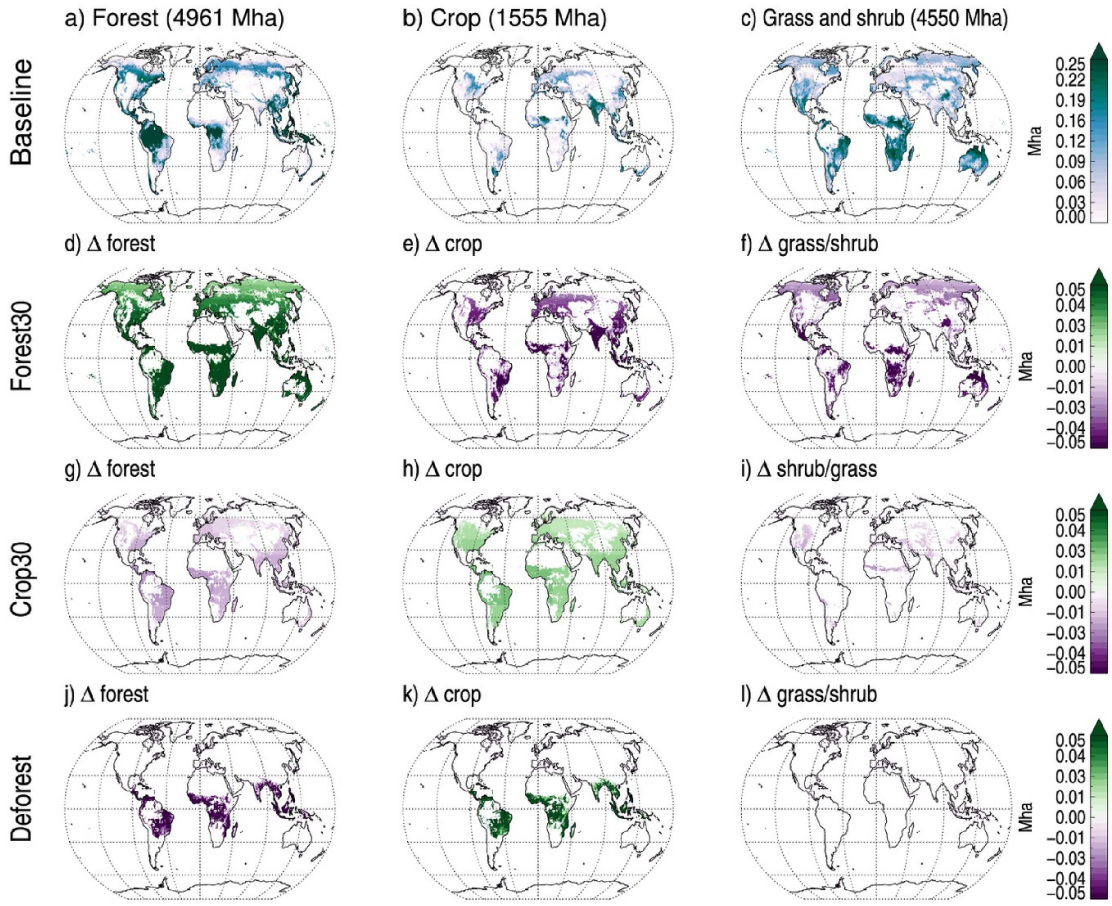

Figure 1. Land cover distributions: cover (Mha) of (a) forests, (b) crops, and (c) grass/shrubs in the baseline model configuration, and the difference in cover of each of these between the baseline and the three experiments Forest30 (d)–(f), Crop30 (g)–(i), and Deforest (j)–(l).

warming scenario. CO_2 is not treated explicitly by the OsloCTM3 but is included as a parameter in the parameterization of isoprene emissions MEGAN2.1. Here we select the SSP1-1.9 (van Vuuren *et al* 2017, Gidden *et al* 2019) and employ the year 2050 emissions and global CO_2 concentrations from this scenario (see figure S3 for selected species).

3. Results

In the following, we describe the global and regional effects of the large-scale vegetation perturbations on simulated isoprene, ozone and biogenic SOA, and the resulting RF.

The OsloCTM3 baseline BVOC emissions and SOA and ozone distributions (figure S4) are broadly consistent with model estimates in the literature (see section SI1 for details). Increasing the global forest cover by 15%, 30% or 50% from the baseline (i.e. experiments Forest15, Forest30 or Forest50) increases the global total isoprene emission by 14%–51% (table 2). Conversely, increasing crop cover at the expense of forest, decreases isoprene emissions, as crops have much lower emission factors. We note that for the same percentage global increase in cover, the absolute changes in total forest and crop area will be very different, due to their different baseline extents (table S1). In particular, a much smaller reduction in forest area is needed to match the respective percentage crop increases compared to the changes in area needed in the corresponding forest increase experiments. The result is changes in total isoprene emissions that are smaller in magnitude in the crop experiments than in the forest experiments.

With higher emissions of isoprene and other BVOCs, the formation of oxidation products and, subsequently, SOA, increases. The global-mean SOA burden is 18%, 37%, and 65% higher in the Forest15, Forest30 and Forest50 experiments, respectively, than in the baseline. In Crop15, Crop30, and Crop50, we find a global-mean reduction in SOA burden of 6%, 12% and 18% following lower BVOC emissions. In Deforest, where the entire 30% increase in global crop cover takes place at the expense of tropical forests with high isoprene emissions, the SOA reduction increases to 20%. In general, the changes in isoprene emissions scale with the magnitude of global change of the respective vegetation type. Hence, we focus on the experiments with 30% increase in the following.

Figures 2(a)–(c) shows total vegetation change and the zonal land average responses of BVOC, SOA and ozone in the Forest30, Crop30 and Deforest

Table 2. Annual global total isoprene emissions and annual, global-mean biogenic SOA burden and tropospheric ozone column in the baseline and sensitivity experiments.

Scenario	Isoprene (Tg yr^{-1})	Ratio	SOA (mg m^{-2})	Ratio	Ozone (DU)	Ratio
Baseline	592	—	1.53	—	33.2	—
Forest15	677	1.14	1.81	1.18	33.2	1.001
Forest30	767	1.30	2.1	1.37	33.2	1.001
Forest50	894	1.51	2.53	1.65	33.2	0.999
Forest30_SSP119anthro	767	1.30	1.89	1.23	27.4	0.82
Forest30_SSP119all	699	1.18	1.78	1.16	27.2	0.82
Crop15	562	0.95	1.44	0.94	33.2	0.999
Crop30	532	0.90	1.35	0.88	33.2	0.998
Crop50	497	0.84	1.25	0.82	33.1	0.997
Crop30_SSP119anthro	532	0.90	1.26	0.82	27.3	0.82
Crop30_SSP119all	485	0.82	1.15	0.75	27.2	0.82
Deforest	482	0.82	1.23	0.80	33.2	0.998

experiments (see figure S5 for maps and for zonal averages for all experiments). Around the tropics (30° S–25° N), the change in isoprene emissions closely follows the change in total forest cover, and the subsequent changes in SOA burden have similar patterns. While the size of the forest cover change in northern hemisphere temperate and boreal regions is similar (or larger) to those in the tropics, their impact on isoprene emissions and SOA burden is smaller than in the tropics. This is as expected given the lower BVOC emission rate and stronger seasonal cycle at higher latitudes. In Forest30, the largest tropospheric ozone increase is seen between 20° N and 50° N, while a reduction occurs over tropical regions (see also figure S5). The opposite pattern is found for Crop30 and Deforest. Over Africa and South America (SAM), ozone also exhibits opposite seasonal responses (not shown). The influence on ozone involves complex chemical processes, with dependence on e.g. background NO_x levels and meteorological conditions. Ozone also has a longer atmospheric lifetime than SOA and atmospheric transport may also influence the simulated changes. The spatial pattern of tropospheric ozone changes therefore shows less direct relationship with the LCC than SOA. We note, however, that the tropospheric ozone changes are relatively small everywhere.

Over key regions (figure 2(d)), such as SAM, Asia (ASIA) and Sub-Saharan Africa, the estimated SOA burdens are 1.1–2.4 mg m^{-2} (i.e. 15%–50%) larger in the Forest30 experiment than the baseline (figure 2(e)). Absolute changes are smaller in higher latitude regions, but still constitute notable relative increases compared to the baseline (31%, 45% and 33% over North America, Europe, and Russia, respectively). In SAF and SAM, the increase in biogenic SOA translates to approximately 15% larger total aerosol load (total here being the sum of fine mode below particles, excluding dust and sea salt). Corresponding numbers for other regions, where SOA contributes less to total aerosol, are 3%–10%. In Crop30, the lower SOA burden translates to 1%–6% lower total aerosol burden, depending on region. Hence, large scale land cover perturbations, especially in the form of increased forest cover, can have notable impacts on the overall aerosol pollution levels. For the tropospheric ozone column, the differences between the baseline and vegetation perturbation experiments are less than than 1% (figure S6). These results assume anthropogenic aerosol and precursor emissions at the present-day level.

Using year 2050 SSP1-1.9 anthropogenic emissions instead (Forest30_SSP119anthro and Crop30_SSP119anthro experiments) has a notable influence on our results. In the case of the Forest30_SSP119anthro and Forest30 experiments, the latitudinal pattern of SOA burden change remains similar in, however, the magnitude of the increase is substantially reduced (figure S5). This is due to the projected decline in primary organic aerosol emissions (figure S3), and hence fewer particles for oxidation products to condense on. In all regions considered here, except SAM and SAF, this effect offsets the impact of the LCC alone, resulting lower SOA burdens in Forest30_SSP119anthro compared to the baseline (figure 2(e), dark green bars). In SAM and SAF, the SOA burden still increases, but less so than if forest increase is the only change taking place. Using year 2050 SSP1-1.9 CO_2 concentration further offsets the SOA burden increase (figure 2(e), light green bars), due to the isoprene inhibition effect (Arneth *et al* 2007). In the case of crop increase, the lower anthropogenic emission enhances the SOA burden reductions already estimated due to the LCC (figure 2(e), dark red bars). These results demonstrates the spatial heterogeneity and complexity of the factors that influence future pathways for SOA. For tropospheric ozone, the change in anthropogenic precursor emissions dominates and result in up to 25% lower concentrations compared to the baseline (figures S5 and S6).

As a 1st order estimate of the climate impact of our large-scale land cover perturbations, we calculate the RF of the changes in SOA and tropospheric ozone (figures 3 and S6). SOA is predominantly scattering and increasing concentrations thus exerts a negative

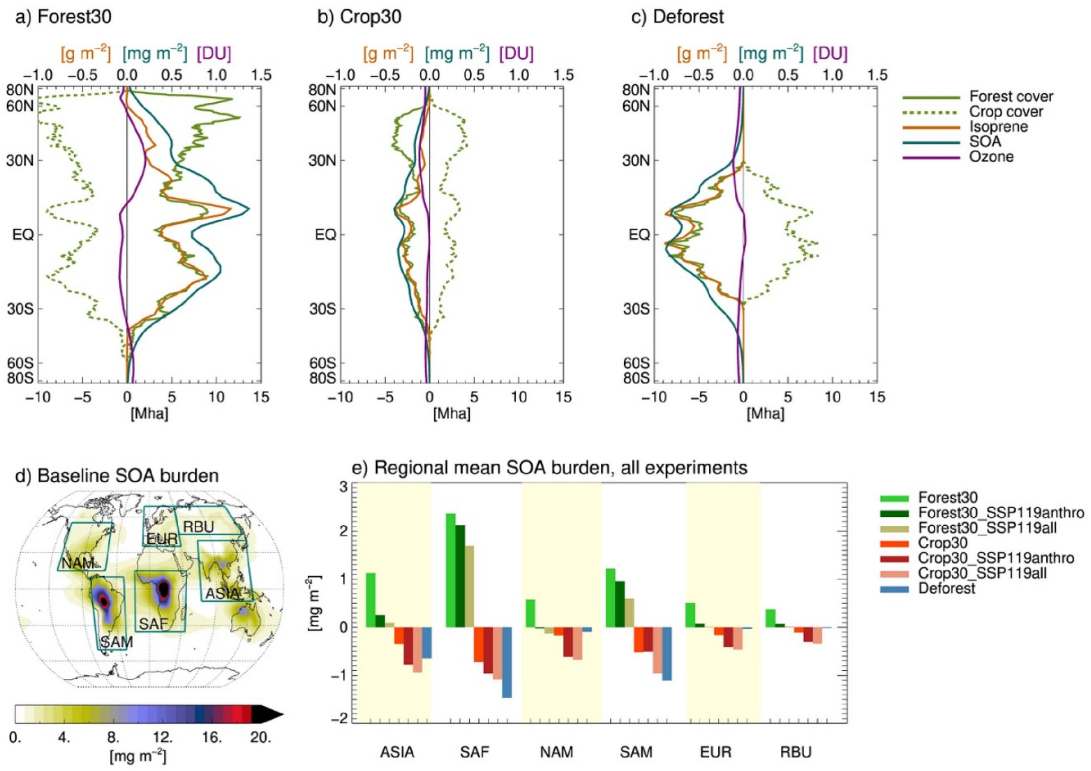

Figure 2. Regional changes: (a)–(c) Zonal, land area averaged change in annual total isoprene emissions, global-mean SOA burden and tropospheric ozone column, and total forest and crop cover, in the experiements Forest30, Crop30 and Deforest compared to the baseline. (d) Annual mean baseline SOA burden. (e) Difference in SOA burden in each experiment compared to the baseline, averaged over the regions shown in panel (d).

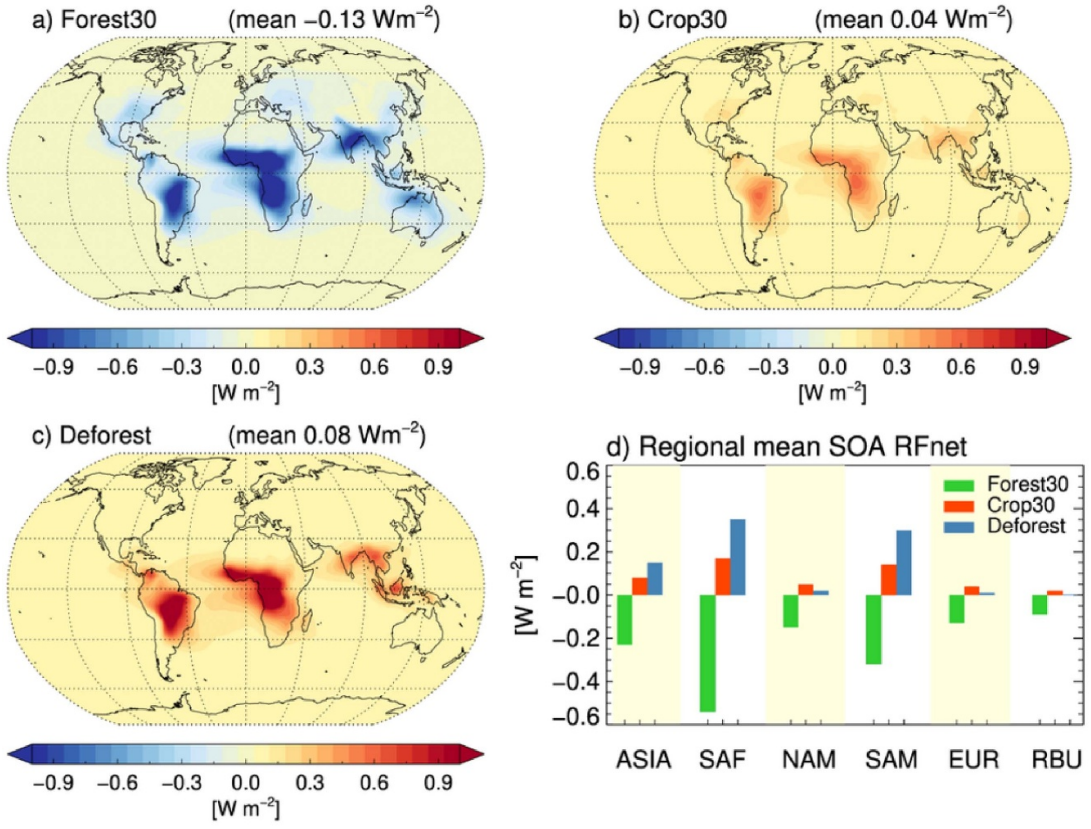

Figure 3. SOA radiative forcing: Net RF (i.e. sum of RFari and RFaci, where RFari is the mean of Oslo-RTM and SOCRATES results) of changes in SOA in the (a) Forest30, (b) Crop30 and (c) Deforest experiments. (d) Corresponding regionally averaged RFnet.

RF. We estimate a global, annual mean net (i.e. sum of RFari and RFaci) SOA RF of -0.13 W m^{-2} for the Forest30 experiment. For Crop30 and Deforest, where aerosol loads are lower than the baseline, we estimate positive RFs of $+0.04$ and $+0.08$ W m^{-2}, respectively. Of this, RFaci constitutes 23%–28%, depending on the experiment. The SOCRATES RFari estimate is 40% stronger than that from Oslo-RTM (figure S7), however, their regional patterns are very similar. The strongest regional net RF in the Forest30 experiment is found over SAF (-0.54 W m^{-2}), followed by SAM (-0.32 W m^{-2}) and ASIA (-0.23 W m^{-2}) (figure 2, table S2). In the Deforest experiment, we estimate the strongest positive RF of 0.35 W m^{-2} over SAF. The radiative efficiency, i.e. RF per SOA burden change, is similar across regions, although somewhat stronger over SAM for RFaci. There are notable regional differences in both sign and magnitude of the ozone RF, in particular in Forest30, where the RF is negative over the tropics and positive over the northern hemisphere (figure S6). Globally, these regional contributions lead to a relatively small tropospheric ozone RF, i.e. 0.001, -0.0017 and -0.0019 W m^{-2} in Forest30, Crop30 and Deforest, respectively.

4. Discussion

Both the present study and previous literature demonstrate that LCC can have important climate impacts through atmospheric chemistry, and emphasize the importance of carefully considering both the characteristics of the LCC in the underlying scenario and the anthropogenic emission trend. While a comprehensive comparison with previous studies is challenging due to differences in methodology and scenarios, the overall responses to LCC in our study are in good agreement with existing literature. Combining satellite retrievals with modeling, Chen *et al* (2018) estimated isoprene emission increases of 5%–10% in response to recent forest cover changes in China and India that are comparable to that in our Forest15 experiment. Using the previous generation global scenarios, the representative concentration pathways (RCPs), Ward *et al* (2014) estimated end-of-century changes in BVOCs attributed to LULCC activities of 6%–16% depending on scenario. Scott *et al* (2018b) suggested that changes in atmospheric chemistry constitute 8% of the net climate LCC impact in an extreme deforestation case. Hantson *et al* (2017) found globally increasing isoprene emissions under RCP4.5 where substantial reforestation efforts were projected, but a decreasing trend in RCP8.5 and RCP2.6 due to a higher degree of deforestation and bioenergy demand, respectively.

SOA formation depends on the background OA abundance. Using an older scenario with increasing anthropogenic emissions, Heald *et al* (2008) projected an increase in global SOA, whereas the strong emission decline projected in recent scenarios give the opposite effect in our study. Biomass burning sources of OA are more uncertain and difficult to project. Additionally, background aerosol levels affect the cloud albedo effect of biogenic SOA (Spracklen and Rap 2013).

Here we have focused on one specific vegetation–climate interaction process. LCC will also influence the energy balance and climate through other biogeophysical and biogeochemical effects such as albedo and evapotranspiration. For instance, looking at historical cropland expansion, Unger (2014) found the global mean RF of albedo changes to be comparable in magnitude to the net effect of LCC-induced changes in atmospheric composition. Moreover, existing literature indicate that LCC may have substantial further local to regional-scale climate implications beyond energy balance perturbations. Studies of LCC, including changes of comparable magnitude to those in our experiments, find important effects on both regional mean and diurnal temperature range, as well as temperature extremes (Alkama and Cescatti 2016, Lejeune *et al* 2017, Hirsch *et al* 2018). These responses cannot be quantified within our current framework but need to be considered for comprehensive assessments of the full consequences of land management and mitigation strategies.

The main motivation behind our study is to explore the impact of large-scale and constrasting LCC and we have thus kept our perturbations idealized and spanning a wide range. To place our numbers into context, our 30% increase in global forest cover corresponds to nearly 1500 Mha (table S1), roughly 3.5 times the extent of forests reported lost through conversion since 1990 (FAO/UNEP 2020). Furthermore, global cropland area is estimated to have increased fivefold (1200 Mha) between 1700 and 1990 (Goldewijk 2001) and by 15% since the 1960s (Arneth *et al* 2019). The latter is similar to our smallest crop perturbation experiment, albeit with regional differences. There is a wide spread in projected future global LCC and temporal evolution in available scenarios. In 89 scenarios from the IAMC 1.5 °C Scenario Explorer that reach 1.5 °C, including with overshoot (Huppman *et al* 2018), changes in total forest (crop) cover from 2010 to 2100 range from a decrease of 240 Mha (550 Mha) to an increase of more than 1700 Mha (900 Mha). With the exception of the Forest50 experiment, individual perturbations in our study fall within these end-of-century ranges.

Furthermore, our experiments are run with present-day meteorology to disentangle the influence of LCC alone. Research has suggested a small but non-negligible warming-induced effect on biogenic emission rates (Unger 2013, Hantson *et al* 2017). For instance, Unger (2013) estimated a 3% increase in global isoprene emissions due to physical climate change alone from 1880 to 2000. Accounting for projected temperature increases could hence increase the BVOC change in our forest increase

experiments or, conversely, reduce the decline in the crop experiments. Moreover, changes in vegetation may themselves affect local temperature and hence emissions. Other influences that can alter the vegetation distribution, and hence BVOCs, include wildfire activity, active species management and changing vegetation in response to climate change. Physical climate change can also alter the distribution of aerosols and ozone via e.g. removal rates and oxidation capacity (Heald *et al* 2008), as well as influence the indirect aerosol effect through changes in clouds. Finally, our modeling framework does no enable us to study feedbacks on plant productivity from changes in SOA and ozone through diffuse radiation or deposition (Rap *et al* 2018). Thus, further studies of LCC in low-warming scenarios are needed to fully understand the interactions with the natural aerosol system and subsequent climate implications.

SOA formation involves complex and interdependent processes with non-linear effects, many still poorly understood (Shrivastava *et al* 2017). For instance, the fraction of BVOCs that is transformed to SOA is suggested to be overestimated in global models due to the coarse resolution and subsequent insufficient level of detail of land surface characteristics and oxidant concentrations. Moreover, not all known oxidation pathways or biogenic precursors are represented in current models, potentially resulting in an underestimation of SOA formation. Finally, the SOA yield has been shown to vary between high and low NO_x environments (Hoyle *et al* 2011). NO_x-dependent yields are not included in the Oslo-CTM3 but could affect the SOA response to LCC under rapidly declining anthropogenic emissions. Combined with the potential changes in SOA that may play out over the coming decades, this underlines the need for further research in this area.

5. Conclusions

The land surface interacts with the atmosphere and climate through a multitude of mechanisms that need to be quantified to assess implications of land-based climate mitigation. Here we have studied one such mechanism: effects of large-scale LCC in line with 1.5 °C warming scenarios on BVOC emissions and abundances of SOA and tropospheric ozone, and the associated RF.

By imposing idealized, contrasting vegetation cover perturbations in a modeling framework, we have demonstrated that LCC, e.g. from afforestation and reforestation or crop expansion, can have substantial regional and global effects on atmospheric composition and energy balance through biosphere-atmosphere interactions involving natural aerosols. We estimate that a 30% increase in global forest cover (corresponding to approximately 1500 Mha), imposed under current climate conditions, atmospheric composition and background emissions, results in 25%–48% higher regional SOA burdens, with the largest changes in SAM and sub-Saharan Africa. In our model, this corresponds to up to 15% increase in total regional biogenic plus anthropogenic aerosol levels. Furthermore, we estimate that these regional SOA changes induce regional RF ranging from -0.09 to -0.54 W m^{-2}. Conversely, increasing global crop cover at the expense of forests and/or grassland reduces BVOCs emissions and SOA burden. For a 30% increase of cropland in tropical regions (460 Mha), we estimate up to 30% lower regional SOA burdens.

Concurrently with LCCs, significant declines in anthropogenic emissions of aerosols and ozone precursors are projected in many low warming scenarios. We find the subsequent reduction in particles for condensation of BVOC oxidation products significantly affects SOA production and burden, in some regions offsetting the effect of increased forest cover on burden. This demonstrates the complex interplay of factors that shape future evolutions of atmospheric SOA. Nevertheless, SOA may come to play a relatively larger role for atmospheric pollution levels in many regions in the future. The impact of vegetation changes alone on tropospheric ozone is relatively small in our experiments and overwhelmed by the impacts of changing anthropogenic emissions.

Our results highlight the importance of considering the biogenic emission pathway in land-climate interaction assessments under low warming scenarios, demonstrating that different strategies for land management and land-based mitigation can have opposing effects even under scenarios with the same long-term effect on global temperature. Further coupled modeling studies, including transient and more realistic land cover evolution, are required to fully quantify and contrast the biogeochemical and biogeophysical climate impacts and feedbacks due to LCC in low warming scenarios.

Data availability statement

The data that support the findings of this study are openly available at the following URL/DOI: 10.6084/m9.figshare.14561826.

Acknowledgments

The authors declare no conflict of interest. CICERO researchers acknowledge funding from the Research Council of Norway (Grant Bio4Clim 244074 and QUIFFiN 254966). We thank Alex Guenther for advice on the MEGAN implementation and Christian Mohr for assistance with input data preparation. Simulations were performed on UNINETT Sigma2—the National Infrastructure for High Performance Computing and Data Storage in Norway—resources (Grant NN9188K).

Author contributions

M T L ran the OsloCTM3 and led the analysis and writing. A S H did the technical implementation of MEGAN in the OsloCTM3. G U M and A R provided RF estimates. B H S had the initial idea for the scope of the study and contributed to the experimental design. All authors participated in the writing.

ORCID iDs

Alexandru Rap https://orcid.org/0000-0002-2319-6769
Bjørn H Samset https://orcid.org/0000-0001-8013-1833

References

Alkama R and Cescatti A 2016 Biophysical climate impacts of recent changes in global forest cover *Science* **351** 600–4
Arneth A, Miller P A, Scholze M, Hickler T, Schurgers G, Smith B and Prentice I C 2007 CO_2 inhibition of global terrestrial isoprene emissions: potential implications for atmospheric chemistry *Geophys. Res. Lett.* **34**
Arneth A *et al* 2019 Framing and context *Climate Change and Land: An IPCC Special Report on Climate Change, Desertification, Land Degradation, Sustainable Land Management, Food Security, and Greenhouse Gas Fluxes in Terrestrial Ecosystems* ed P R Shukla, J Skea, E Calvo Buendia, V Masson-Delmotte, H-O Pörtner, D C Roberts, P Zhai, R Slade, S Connors, R van Diemen, M Ferrat, E Haughey, S Luz, S Neogi, M Pathak, J Petzold, J Portugal Pereira, P Vyas, E Huntley, K Kissick, M Belkacemi and J Malley accepted (https://www.ipcc.ch/site/assets/uploads/sites/4/2019/12/04_Chapter-1.pdf)
Bala G, Caldeira K, Wickett M, Phillips T J, Lobell D B, Delire C and Mirin A 2007 Combined climate and carbon-cycle effects of large-scale deforestation *Proc. Natl Acad. Sci.* **104** 6550–5
Bellouin N, Rae J, Jones A, Johnson C, Haywood J and Boucher O 2011 Aerosol forcing in the climate model intercomparison project (CMIP5) simulations by HadGEM2-ES and the role of ammonium nitrate *J. Geophys. Res.* **116**
Berntsen T K and Isaksen I S A 1997 A global three-dimensional chemical transport model for the troposphere: 1. Model description and CO and ozone results *J. Geophys. Res.* **102** 21239–80
Bertram C, Luderer G, Popp A, Minx J C, Lamb W F, Stevanović M, Humpenöder F, Giannousakis A and Kriegler E 2018 Targeted policies can compensate most of the increased sustainability risks in 1.5 °C mitigation scenarios *Environ. Res. Lett.* **13** 064038
Carslaw K S *et al* 2013 Large contribution of natural aerosols to uncertainty in indirect forcing *Nature* **503** 67
Carslaw K S, Boucher O, Spracklen D V, Mann G W, Rae J G L, Woodward S and Kulmala M 2010 A review of natural aerosol interactions and feedbacks within the Earth system *Atmos. Chem. Phys.* **10** 1701–37
Chen W H, Guenther A B, Wang X M, Chen Y H, Gu D S, Chang M, Zhou S Z, Wu L L and Zhang Y Q 2018 Regional to global biogenic isoprene emission responses to changes in vegetation from 2000 to 2015 *J. Geophys. Res.* **123** 3757–71
Chung S H and Seinfeld J H 2002 Global distribution and climate forcing of carbonaceous aerosols *J. Geophys. Res.* **107** AAC 14–11-AAC 14–33
Claeys M *et al* 2004 Formation of secondary organic aerosols through photooxidation of isoprene *Science* **303** 1173–6
D'Andrea S D, Häkkinen S A K, Westervelt D M, Kuang C, Levin E J T, Kanawade V P, Leaitch W R, Spracklen D V, Riipinen I and Pierce J R 2013 Understanding global secondary organic aerosol amount and size-resolved condensational behavior *Atmos. Chem. Phys.* **13** 11519–34
Doelman J C *et al* 2018 Exploring SSP land-use dynamics using the IMAGE model: regional and gridded scenarios of land-use change and land-based climate change mitigation *Glob. Environ. Change* **48** 119–35
Edwards J M and Slingo A 1996 Studies with a flexible new radiation code. I: choosing a configuration for a large-scale model *Q. J. R. Meteorol. Soc.* **122** 689–719
FAO/UNEP 2020 The state of the world's forests 2020. Forests, biodiversity and people (Rome) (https://doi.org/10.4060/ca8642en)
Ghimire B, Williams C A, Masek J, Gao F, Wang Z, Schaaf C and He T 2014 Global albedo change and radiative cooling from anthropogenic land cover change, 1700–2005 based on MODIS, land use harmonization, radiative kernels, and reanalysis *Geophys. Res. Lett.* **41** 9087–96
Gidden M J *et al* 2019 Global emissions pathways under different socioeconomic scenarios for use in CMIP6: a dataset of harmonized emissions trajectories through the end of the century *Geosci. Model Dev.* **12** 1443–75
Goldewijk K K 2001 Estimating global land use change over the past 300 years: the HYDE database *Glob. Biogeochem. Cycles* **15** 417–33
Guenther A B, Jiang X, Heald C L, Sakulyanontvittaya T, Duhl T, Emmons L K and Wang X 2012 The model of emissions of gases and aerosols from nature version 2.1 (MEGAN2.1): an extended and updated framework for modeling biogenic emissions *Geosci. Model Dev.* **5** 1471–92
Guenther A, Karl T, Harley P, Wiedinmyer C, Palmer P I and Geron C 2006 Estimates of global terrestrial isoprene emissions using MEGAN (model of emissions of gases and aerosols from nature) *Atmos. Chem. Phys.* **6** 3181–210
Hantson S, Knorr W, Schurgers G, Pugh T A M and Arneth A 2017 Global isoprene and monoterpene emissions under changing climate, vegetation, CO_2 and land use *Atmos. Environ.* **155** 35–45
Harper A B *et al* 2018 Land-use emissions play a critical role in land-based mitigation for Paris climate targets *Nat. Commun.* **9** 2938
Heald C L *et al* 2008 Predicted change in global secondary organic aerosol concentrations in response to future climate, emissions, and land use change *J. Geophys. Res.* **113**
Hirsch A L *et al* 2018 Biogeophysical impacts of land-use change on climate extremes in low-emission scenarios: results from HAPPI-land *Earth's Future* **6** 396–409
Hoesly R M *et al* 2018 Historical (1750–2014) anthropogenic emissions of reactive gases and aerosols from the community emission data system (CEDS) *Geosci. Model Dev.* **2018** 369–408
Hoyle C R *et al* 2011 A review of the anthropogenic influence on biogenic secondary organic aerosol *Atmos. Chem. Phys.* **11** 321–43
Hoyle C R, Berntsen T, Myhre G and Isaksen I S A 2007 Secondary organic aerosol in the global aerosol-chemical transport model Oslo CTM2 *Atmos. Chem. Phys.* **7** 5675–94
Huppman D *et al* 2018 IAMC 1.5 °C scenario explorer and data hosted by IIASA *Integrated Assessment Modeling Consortium and International Institute for Applied Systems Analysis, 2018* (https://doi.org/10.5281/zenodo.3363345)
Jimenez J L *et al* 2009 Evolution of organic aerosols in the atmosphere *Science* **326** 1525–9
Kanakidou M *et al* 2005 Organic aerosol and global climate modelling: a review *Atmos. Chem. Phys.* **5** 1053–123
Lawrence D M *et al* 2011 Parameterization improvements and functional and structural advances in version 4 of the community land model *J. Adv. Model. Earth Syst.* **3**
Lejeune Q, Seneviratne S I and Davin E L 2017 Historical land-cover change impacts on climate: comparative

assessment of LUCID and CMIP5 multimodel experiments *J. Clim.* **30** 1439–59
Lund M T, Myhre G, Haslerud A S, Skeie R B, Griesfeller J, Platt S M, Kumar R, Myhre C L and Schulz M 2018 Concentrations and radiative forcing of anthropogenic aerosols from 1750 to 2014 simulated with the Oslo CTM3 and CEDS emission inventory *Geosci. Model Dev.* **11** 4909–31
Mahmood R *et al* 2014 Land cover changes and their biogeophysical effects on climate *Int. J. Climatol.* **34** 929–53
Myhre G *et al* 2017 Multi-model simulations of aerosol and ozone radiative forcing due to anthropogenic emission changes during the period 1990–2015 *Atmos. Chem. Phys.* **17** 2709–20
O'Neill B C, Kriegler E, Riahi K, Ebi K L, Hallegatte S, Carter T R, Mathur R and van Vuuren D P 2014 A new scenario framework for climate change research: the concept of shared socioeconomic pathways *Clim. Change* **122** 387–400
Paasonen P *et al* 2013 Warming-induced increase in aerosol number concentration likely to moderate climate change *Nat. Geosci.* **6** 438–42
Pacifico F, Harrison S P, Jones C D and Sitch S 2009 Isoprene emissions and climate *Atmos. Environ.* **43** 6121–35
Pongratz J, Reick C H, Raddatz T and Claussen M 2010 Biogeophysical versus biogeochemical climate response to historical anthropogenic land cover change *Geophys. Res. Lett.* **37**
Popp A *et al* 2017 Land-use futures in the shared socio-economic pathways *Glob. Environ. Change* **42** 331–45
Quaas J, Boucher O and Lohmann U 2006 Constraining the total aerosol indirect effect in the LMDZ and ECHAM4 GCMs using MODIS satellite data *Atmos. Chem. Phys.* **6** 947–55
Rap A *et al* 2018 Enhanced global primary production by biogenic aerosol via diffuse radiation fertilization *Nat. Geosci.* **11** 640–4
Rap A, Richards N A D, Forster P M, Monks S A, Arnold S R and Chipperfield M P 2015 Satellite constraint on the tropospheric ozone radiative effect *Geophys. Res. Lett.* **42** 5074–81
Rap A, Scott C E, Spracklen D V, Bellouin N, Forster P M, Carslaw K S, Schmidt A and Mann G 2013 Natural aerosol direct and indirect radiative effects *Geophys. Res. Lett.* **40** 3297–301
Roe S *et al* 2019 Contribution of the land sector to a 1.5 °C world *Nat. Clim. Change* **9** 817–28
Rogelj J *et al* 2018 Mitigation pathways compatible with 1.5 °C in the context of sustainable development *Global Warming of 1.5 °C. An IPCC Special Report on the Impacts of Global Warming of 1.5 °C above Pre-industrial Levels and Related Global Greenhouse Gas Emission Pathways, in the Context of Strengthening the Global Response to the Threat of Climate Change, Sustainable Development, and Efforts to Eradicate Poverty* ed V Masson-Delmotte, P Zhai, H-O Pörtner, D Roberts, J Skea, P R Shukla, A Pirani, W Moufouma-Okia, C Péan, R Pidcock, S Connors, J B R Matthews, Y Chen, X Zhou, M I Gomis, E Lonnoy, T Maycock, M Tignor and T Waterfield accepted (https://www.ipcc.ch/sr15/chapter/chapter-2)
Scott C E *et al* 2018b Impact on short-lived climate forcers increases projected warming due to deforestation *Nat. Commun.* **9** 157
Scott C E, Arnold S R, Monks S A, Asmi A, Paasonen P and Spracklen D V 2018a Substantial large-scale feedbacks between natural aerosols and climate *Nat. Geosci.* **11** 44–48
Scott C E, Monks S A, Spracklen D V, Arnold S R, Forster P M, Rap A, Carslaw K S, Chipperfield M P, Reddington C L S and Wilson C 2017 Impact on short-lived climate forcers (SLCFs) from a realistic land-use change scenario via changes in biogenic emissions *Faraday Discuss.* **200** 101–20
Shrivastava M *et al* 2017 Recent advances in understanding secondary organic aerosol: implications for global climate forcing *Rev. Geophys.* **55** 509–59
Søvde O A, Prather M J, Isaksen I S A, Berntsen T K, Stordal F, Zhu X, Holmes C D and Hsu J 2012 The chemical transport model Oslo CTM3 *Geosci. Model Dev.* **5** 1441–69
Sporre M K, Blichner S M, Schrödner R, Karset I H H, Berntsen T K, van Noije T, Bergman T, O'Donnell D and Makkonen R 2020 Large difference in aerosol radiative effects from BVOC-SOA treatment in three Earth system models *Atmos. Chem. Phys.* **20** 8953–73
Spracklen D V and Rap A 2013 Natural aerosol–climate feedbacks suppressed by anthropogenic aerosol *Geophys. Res. Lett.* **40** 5316–9
Stamnes K, Tsay S C, Wiscombe W and Jayaweera K 1988 Numerically stable algorithm for discrete-ordinate-method radiative transfer in multiple scattering and emitting layered media *Appl. Opt.* **27** 2502–9
Tai A P K, Mickley L J, Heald C L and Wu S 2013 Effect of CO_2 inhibition on biogenic isoprene emission: implications for air quality under 2000–2050 changes in climate, vegetation, and land use *Geophys. Res. Lett.* **40** 3479–83
Thornhill G *et al* 2021 Climate-driven chemistry and aerosol feedbacks in CMIP6 Earth system models *Atmos. Chem. Phys.* **21** 1105–26
Unger N 2013 Isoprene emission variability through the twentieth century *J. Geophys. Res.* **118** 13–606
Unger N 2014 Human land-use-driven reduction of forest volatiles cools global climate *Nat. Clim. Change* **4** 907
van Marle M J E *et al* 2017 Historic global biomass burning emissions for CMIP6 (BB4CMIP) based on merging satellite observations with proxies and fire models (1750–2015) *Geosci. Model Dev.* **10** 3329–57
van Vuuren D P *et al* 2017 Energy, land-use and greenhouse gas emissions trajectories under a green growth paradigm *Glob. Environ. Change* **42** 237–50
Ward D S, Mahowald N M and Kloster S 2014 Potential climate forcing of land use and land cover change *Atmos. Chem. Phys.* **14** 12701–24
Zhu J, Penner J E, Yu F, Sillman S, Andreae M O and Coe H 2019 Decrease in radiative forcing by organic aerosol nucleation, climate, and land use change *Nat. Commun.* **10** 423
Zhu Z, Bi J, Pan Y, Ganguly S, Anav A, Xu L, Samanta A, Piao S, Nemani R R and Myneni R B 2013 Global data sets of vegetation leaf area index (LAI)3g and fraction of photosynthetically active radiation (FPAR)3g derived from global inventory modeling and mapping studies (GIMMS) normalized difference vegetation index (NDVI3g) for the period 1981–2011 *Remote Sens.* **5** 927–48